

# Mn - DPDP

:

1

2

2

3

3

(Mn - DPDP)

: 1.5 T

23 32

(spin echo, SE) 4가 (gradient echo, GRE) T1

: 2 (2 - dimensional fast low angle shot, 2D FLASH),

3 (3 - dimensional fast low angle shot reconstruction, 3D FLASH)

(fat saturation).

(Signal to Noise ratio, SNR) (Percentage

of Signal Enhancement ratio, PSER) (Contrast

to Noise ratio, CNR) , 가

: SNR CNR

Mn - DPDP 가 ( $p < 0.05$ ), PSER CNR

3D FLASH, 2D FLASH FS 가 , SE

가 ( $p < 0.05$ ). CNR ,

100% CNR 가 SE

SE 2D FLASH FS 가

2D FLASH FS GRE SE , SE

( $p < 0.05$ ).

가 가 GRE SE

: , 2D 3D FLASH SE .

(CT) (MRI) , 가 , 가

MRI가 CT

(2, 3).

CT (1). , , 가

CT (characterization) MRI 가

(1, 4). ,

1

2

3

2001 5 29 2001 11 15 . 6), (5,

367

: Mn-DPDP

(superparamagnetic iron oxide, SPIO) (paramagnetic hepatobiliary contrast agent)가 (7).

Manganese(II) N,N'-dipyridoxalethylenediamine - N,N'-diacetate 5,5"-bis(phosphate) (Mn-DPDP)

T1 T1 가 .

. Wang (8) T1 (gradient echo, GRE) T1 (spin echo, SE)

, Slater (9) 가 T1 GRE T1

SE 가 T1 GRE (section) (8 - 10 mm),

(intersection gaps) (partial volume artifact)

(reformation) , (volume)

metric) 가 (10-13). Mn-DPDP GRE SE 가

4가 GRE 5가 T1 : 2 (2 - dimensional fast low angle shot, 2D FLASH), 3 (3 - dimensional fast

low angle shot reconstruction, 3D FLASH) (fat saturation). 2 7 mm

, 3 2.3 mm 7 mm FOV

(240 - 270 mm) x (300 - 360 mm) : 1)

SE : repetition time (TR)/echo time (TE)=400 - 600/14

15, =90°; 2 (signal acquisition; SA), (acquisition time; TA)=5 , =125 x 256,

2) 2 (2D FLASH): TR/TE=128/4.1 6.0, =70° 80°; 1 , TA=17 , =115 x 256, 3) 3 (3D

FLASH): TR/TE=3.8/1.8, =15°; 1 , TA=20 , =115 x 256 가

Mn-DPDP (Mangafodipir trisodium, Teslascan , Nycomed, Amersham, Oslo, Norway) 50 ml

ml 10 µmol (7.57mg) Mn-DPDP 5 µmol/kg 20

2

MR

CT Mn-DPDP MRI 33 ( 27 , 6 , 39 - 79 , 56 )

23 가 MRI Mn-DPDP

3 (region of interest, ROI) (phase

(n=2), (n=21), (n=5), encoding direction)

(n=2), (n=2), (n=2) (parameter)

MRI 1 (n=3) (Signal to Noise ratio, SNR),

, CT, MRI, (Contrast to Noise ratio, CNR)

CT (tumor marker study) . CNR , (Percent - age of

CT MR Signal Enhancement ratio, PSER) . parame -

1. SNR: ROI ter

2. CNR: ( - )/

3. CNR: | -



GRE ( $p < 0.05$ ). (Table 4).  
SE, GRE ( $p < 0.05$ ),  
SE 2D FLASH FS ( $p < 0.05$ ). GRE (Fig. 3).

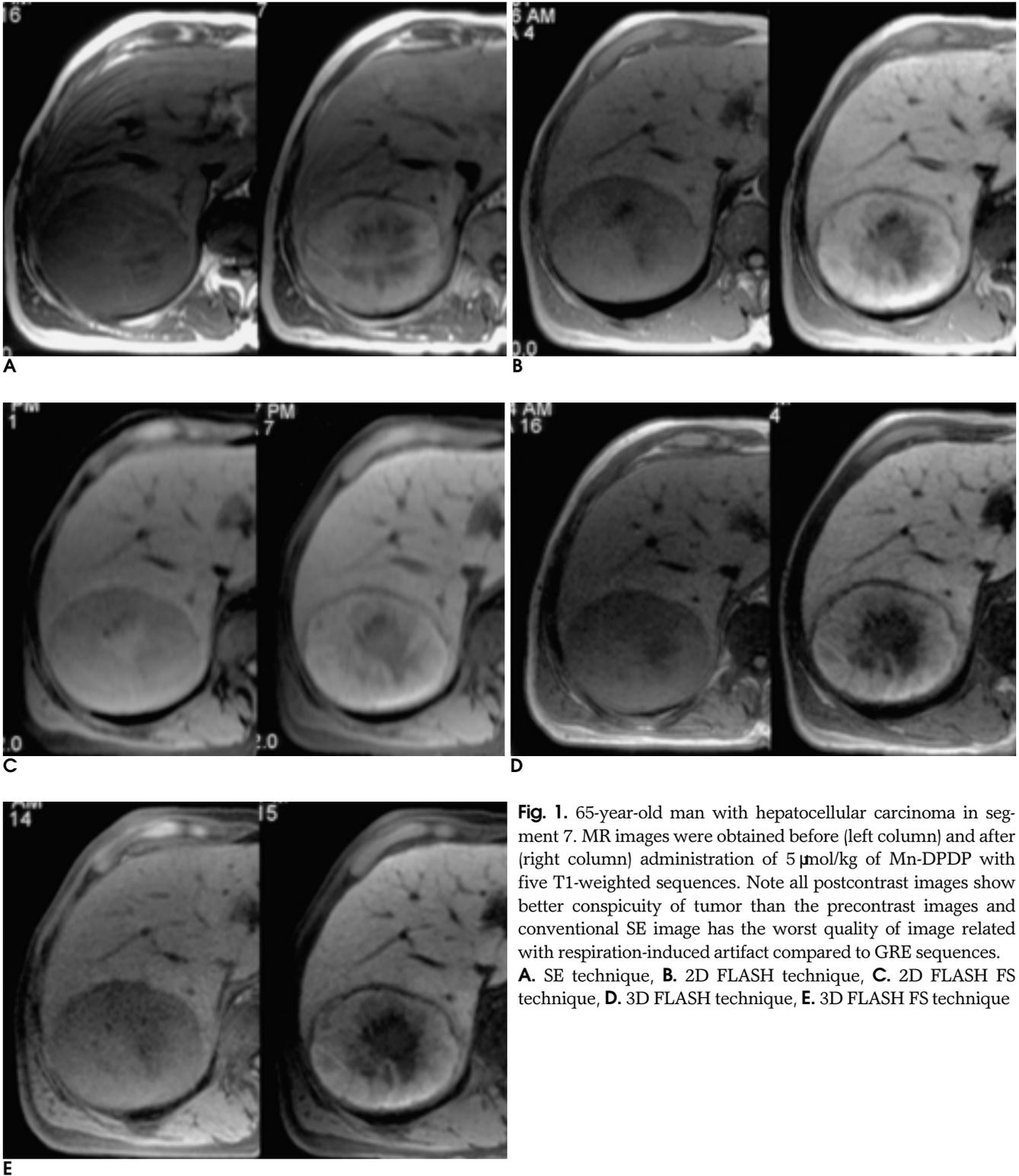


**Fig. 1.** 65-year-old man with hepatocellular carcinoma in segment 7. MR images were obtained before (left column) and after (right column) administration of 5  $\mu\text{mol/kg}$  of Mn-DPDP with five T1-weighted sequences. Note all postcontrast images show better conspicuity of tumor than the precontrast images and conventional SE image has the worst quality of image related with respiration-induced artifact compared to GRE sequences. **A.** SE technique, **B.** 2D FLASH technique, **C.** 2D FLASH FS technique, **D.** 3D FLASH technique, **E.** 3D FLASH FS technique

(Fig. 4): GRE 50% (16/32) SE 56%(18/32). 32 97%(31/32), SE GRE (p < 0.05).

CNR SNR 가 (15-17). Mn-DPDP DPDP가 (Mn<sup>2+</sup>) T1

**Table 2.** Absolute Tumor-to-Liver Contrast-to-Noise Ratio of Focal Hepatic Tumor

MR Pulse Sequence	Absolute CNR		Rank
	Precontrast	Postcontrast*	
2D FLASH	14.64 ± 8.77	32.21 ± 22.15	2 <sup>‡</sup>
2D FLASH FS	13.10 ± 10.28	34.46 ± 20.59	1 <sup>†</sup>
3D FLASH	7.46 ± 5.06	15.08 ± 12.42	5
3D FLASH FS	12.45 ± 7.21	25.13 ± 15.67	3 <sup>‡</sup>
SE	16.98 ± 15.26	20.86 ± 13.50	4

Note - Numbers are mean ± standard deviation.  
 \* ; Every mean absolute CNRs of postcontrast image is higher (p < 0.05) than those of precontrast image of tumor.  
 †; The absolute CNRs of 2D FLASH FS image is the highest of other images.  
 ‡; These two images have higher absolute CNR than SE image significantly (p < 0.05).

**Table 3.** Nonabsolute Tumor-to-Liver Contrast-to-Noise Ratio and Percentage of Signal Enhancement Ratio of Focal Hepatic Tumors

Tumor	Nonabsolute CNR		PSER	Rank
	Precontrast	Postcontrast		
FNH <sup>‡</sup>	5.21 ± 9.38	33.87 ± 14.05*	131 ± 57.98	1 <sup>†</sup>
HCC <sup>‡</sup>	- 0.39 ± 16.86	6.45 ± 7.72	83 ± 43.57	2 <sup>†</sup>
Hemangioma	- 31.38 ± 4.95	- 61.36 ± 34.71*	12 ± 21.21	3
Metastasis	- 12.81 ± 5.70	- 45.24 ± 3.56*	8.67 ± 1.53	4
Cholangiocarcinoma	- 15.51 ± 0.48	- 30.48 ± 2.29*	3.5 ± 6.36	5

Note - Numbers are mean ± standard deviation.  
 \* ; These four tumors have higher nonabsolute CNR than HCC significantly (p < 0.05).  
 †; These two tumors have higher PSER than other tumors significantly (p < 0.05) except hemangioma.  
 ‡; FNH is the abbreviation of focal nodular hyperplasia and HCC is that of hepatocellular carcinoma.

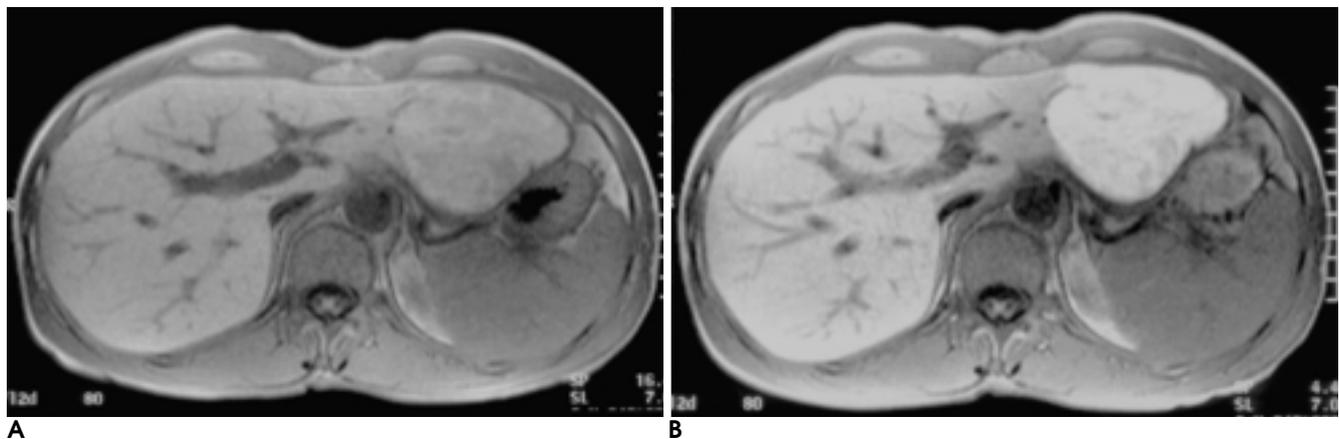


**Fig. 2.** 48 year-old man with focal nodular hyperplasia in lateral segment.  
**A.** Unenhanced 2D FLASH FS image depicts a lesion that is subtly increased in signal intensity compared with normal hepatic parenchyma.  
**B.** Mn-DPDP enhanced image, obtained with identical imaging parameters as used in image A, demonstrates homogeneous enhancement of the lesion

: Mn-DPDP

가 (18, 19). Mn-DPDP T1 가 (21, Mn-DPDP) 가 (22). Murakami (22) MRI 가 PSER 가 (p < 0.05). CNR Mn-DPDP (Fig. 3). 100% CNR 가 Mn-DPDP MR 가 Burkill (20) Mn-DPDP Mn-DPDP 가 PSER CNR 가가

**Table 4.** Tumor Conspicuity, Image Artifact and Tumor Delineation of Various Sequences

MR Pulse Sequence	Lesion Conspicuity		Image Artifact		Mass Delineation	
	pre	post	pre	post	pre	post
2D FLASH	4.1 ± 0.9	4.8 ± 0.5*	4.7 ± 0.5	4.9 ± 0.3 <sup>†</sup>	4.0 ± 0.8	4.5 ± 0.7 <sup>‡</sup>
2D FLASH FS	3.9 ± 1.1	4.6 ± 0.7*	4.8 ± 0.4	4.9 ± 0.3 <sup>†</sup>	3.6 ± 1.1	4.1 ± 0.8
3D FLASH	3.9 ± 1.0	4.9 ± 0.3*	4.1 ± 0.6	4.7 ± 0.5 <sup>†</sup>	3.8 ± 0.9	4.9 ± 0.3 <sup>‡</sup>
3D FLASH FS	4.0 ± 0.8	4.9 ± 0.3*	4.6 ± 0.5	4.7 ± 0.5 <sup>†</sup>	3.9 ± 0.6	4.8 ± 0.4 <sup>‡</sup>
SE	3.0 ± 1.0	3.7 ± 1.2	2.8 ± 0.6	3.0 ± 0.3	2.7 ± 0.9	3.3 ± 0.9

Note - Numbers are mean ± standard deviation.

\* † ‡; Significant difference with postcontrast image of other sequences (p < 0.05).

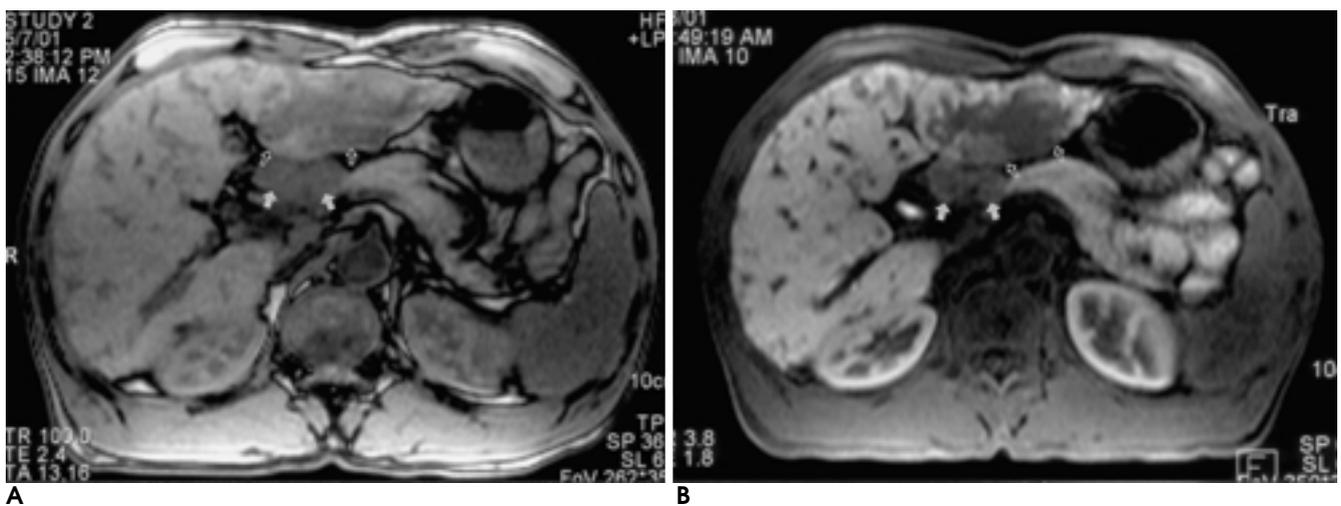


**Fig. 3.** 61 year-old man with hepatocellular carcinoma.

**A.** Unenhanced 2D FLASH image shows a irregular, oval shaped hypointense mass (open arrows) in the left lobe of the liver and an enlarged hilar lymph node (arrows) with hypointensity.

**B.** After administration of Mn-DPDP, 3D FLASH FS image shows an inhomogeneously enhanced hepatic mass (open arrows) and enhancing hilar lymph node (arrows).

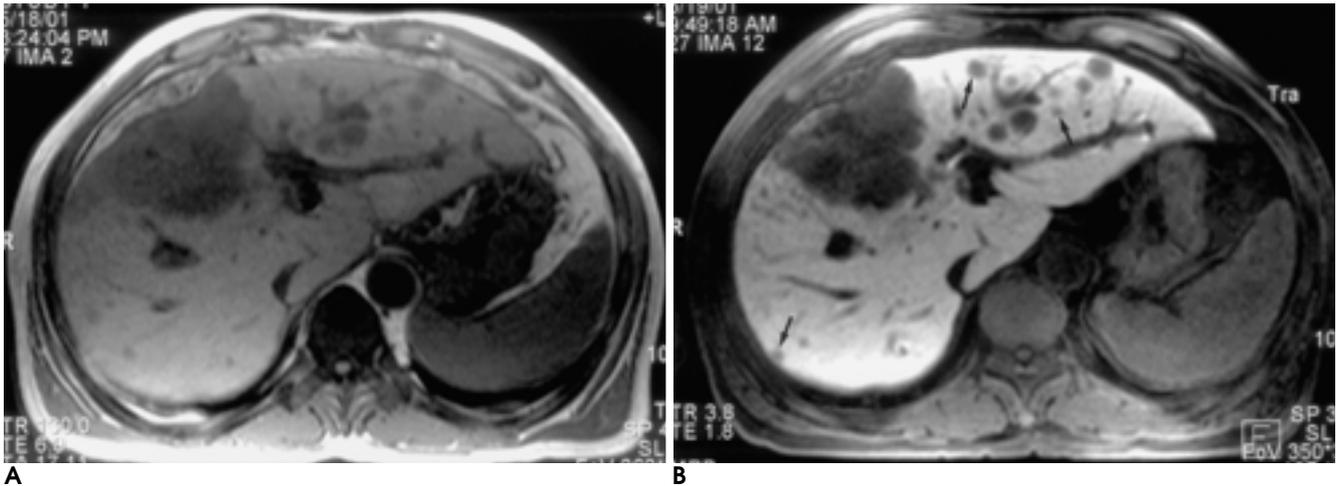


**Fig. 4.** 57 year-old man with peripheral cholangiocarcinoma accompanied with intrahepatic metastases.  
**A.** Unenhanced 2D FLASH image reveals a main mass with a few metastatic nodules in the left lobe of the liver.  
**B.** On Mn-DPDP enhanced 3D FLASH FS image, the main mass is more conspicuous and more nodules (arrows) are seen in the adjacent parenchyma of the right lobe and the left lobe.

가 CNR 가 , 2.3 ms  
 CNR T1  
 Mn - DPDP PSER  
 가  
 3D FLASH CNR (reformation)  
 2D FLASH FS 가 (pixel) 가 (volu -  
 SE metric) 가 (10 - 13).  
 Mn - DPDP , SE 3D FLASH  
 GRE  
 Hamm (19) Mn - DPDP  
 SE GRE  
 SE SE  
 SE 2D FLASH FS Mn - DPDP MR  
 가 GRE 3D FLASH 가  
 GRE SE (23). , 3D FLASH  
 GRE SE PSER CNR MR Mn - DPDP  
 가  
 Mn - DPDP MR GRE SE Mn - DPDP  
 Mn - DPDP MR GRE SE Mn - DPDP  
 GRE SE GRE SE GRE 가 2

## Acknowledgement: MR

1. Federele M, Chezmar J, et al. Efficacy and safety of mangofodipir trisodium(MnDPDP) injection for hepatic MRI in adults: results of the U.S. multicenter phase III clinical trials. Efficacy of early imaging. *J Magn Reson Imaging* 2000;12:689-701
2. Weissleder R, Bogdanor A, Papisov M. Drug targeting in magnetic resonance imaging. *Magn Reson Q* 1992;8:55-63
3. Brasch RC. New directions in the development of MR imaging contrast media. *Radiology* 1992;183:1-11
4. Heiken JP, Brink JA, McClennan BL, et al. Dynamic contrast-enhanced CT of the liver: comparison of contrast medium injection rates and uniphasic and biphasic injection protocols. *Radiology* 1993;187:327-331
5. Mitchell KG. Hepatobiliary contrast material. A magic bullet for sensitivity and specificity. *Radiology* 1993; 188: 21-23
6. Weissleder R. Liver MR imaging with iron oxides: toward consensus and clinical practice[editorial:comment]. *Radiology* 1994;193: 593-595
7. Bernardino ME, Young SW, et al. Hepatic MR Imaging with Mn-DPDP: safety, image quality, and sensitivity. *Radiology* 1992;183: 53-58
8. Wang C, Ahlstrom H, Ekholm S, et al. Diagnostic efficacy of MnDPDP in MR imaging of the liver: a phase III multicentre study. *Acta Radiol* 1997;38:643-649
9. Slater GJ, Saini S, Mayo-smith WW, et al. Mn-DPDP enhanced MR imaging of the liver: analysis of pulse sequence performance. *Clin Radiol* 1996;51:484-486
10. Lee VS, Lavelle MT, Rofsky NM, et al. Hepatic MR imaging with a dynamic contrast-enhanced isotropic volumetric interpolated breath-hold examination: feasibility, reproducibility, and technical quality. *Radiology* 2000;215:365-372
11. Lavelle MT, Lee VS, Rofsky NM, et al. Dynamic contrast-enhanced three-dimensional MR imaging of liver parenchyma: source images and angiographic reconstructions to define hepatic arterial anatomy. *Radiology* 2001;218:389-394
12. Hurst GC, Hua J, Simonetti OP, Duerk JI. Signal-to-noise, resolution, and bias function analysis of asymmetric sampling with zero-padded magnitude FT reconstruction. *Magn Reson Med* 1992;27: 247-269
13. Du YP, Parker KL, Davis WL, Cao G. Reduction of partial-volume artifacts with zero-filled interpolation in three-dimensional MR angiography. *J Magn Reson Imaging* 1994;4:733-741
14. Foster DO, Lardy HA, Ray PE, Johnston JB. Alteration of rat liver phosphoenolpyruvate carboxykinase activity by L-tryptophan in vivo and metals in vitro. *Biochemistry* 1967;6:2120
15. Tsang YM, Stark DD, Chen MC, Weissleder R, et al. Hepatic micrometastases in the rat: ferrite-enhanced MR imaging. *Radiology* 1988;167:21-24
16. Stark DD, Weissleder R, Elizondo G, et al. Superparamagnetic iron oxide: clinical application as a contrast agent for MR imaging of the liver. *Radiology* 1988;168:297-301
17. Marchal G, Hecke PV, Demaerel P, et al. Detection of liver metastases with superparamagnetic iron oxide in 15 patients: results of MR imaging at 1.5 tesla. *AJR Am J Roentgenol* 1989;152:771-775
18. Rummeny EJ, Torres CH, Kurdziel JC, et al. MnDPDP for MR imaging of the liver. Results of an independent image evaluation of the European phase III studies. *Acta Radiol* 1997;38:638-642
19. Hamm B, Vogl TJ, Branding G, et al. Focal liver lesions: MR imaging with Mn-DPDP -initial clinical results in 40 patients. *Radiology* 1992;182:167-174
20. Burkill GC, Mannion EM, Healy JC. Lymph node enhancement at MRI with Mn-DPDP in primary hepatocellular carcinoma. *Clin Radiol* 2001;56:67-71
21. Rofsky NM, Lee VS, Laub G, et al. Abdominal MR imaging with a volumetric interpolated breath-hold examination. *Radiology* 1999; 212:876-884
22. Murakami T, Baron RL, Peterson M, et al. Hepatocellular carcinoma : MR imaging with Mangafodipir Trisodium (Mn-DPDP). *Radiology* 1996;200:69-77
23. Vitellas KM, El-Dieb A, Vasawani K, et al. Detection of bile duct leaks using MR cholangiography with Mangafodipir Trisodium. *J Comput Assist Tomogr* 2001;25:102-105

## Mn-DPDP - enhanced MR Imaging: the Optimal Pulse Sequence for Detection of Focal Hepatic Tumor<sup>1</sup>

Ji Hyun Youk, M.D., Jeong Min Lee, M.D., In Hwan Kim, M.D.,  
Gyung Ho Chung, M.D., Seung Ok Lee, M.D.<sup>2</sup>, Dae Kon Kim, M.D.<sup>2</sup>,  
Hee Cheol You, M.D.<sup>3</sup>, Back Hwan Cho, M.D.<sup>3</sup>, Chong Soo Kim, M.D.

<sup>1</sup>Department of Radiology, Chonbuk National University Hospital

<sup>2</sup>Department of Internal Medicine, Division of Hepatogastroenterology, Chonbuk National University Hospital

<sup>3</sup>Department of General Surgery, Chonbuk National University Hospital

**Purpose:** To assess the diagnostic value of Mn-DPDP for the detection of focal hepatic tumors on MR images and to determine the optimal pulse sequence to maximize its effect.

**Materials and Methods:** Twenty-three patients with 32 focal hepatic tumors were examined by means of 1.5-T MRI. Before and after the intravenous administration of Mn-DPDP, five pulse sequences were used to obtain T1-weighted images: two-dimensional fast low-angle shot (2D FLASH) with/without fat saturation (FS), spin-echo (SE), and three-dimensional fast low angle shot reconstruction (3D FLASH) with/without FS. Quantitative assessment involved determination of the signal-to-noise ratio (SNR) of the liver and the tumor, the percentage signal enhancement ratio (PSER) of the liver, and tumor-to-liver contrast to noise ratio (CNR). Pulse sequences were also evaluated subjectively for tumor conspicuity, delineation, and image artifact. In addition, two experienced radiologists compared tumor detection rates between precontrast and postcontrast images.

**Results:** Mn-DPDP had a marked effect on liver SNR and absolute CNR at all pulse sequences ( $p < 0.05$ ). On postcontrast images, PSER and absolute CNR of the liver were highest at 3D FLASH and 2D FLASH FS, respectively, and significantly higher at GRE than at SE ( $p < 0.05$ ). On postcontrast images, the CNR of focal nodular hyperplasia and hepatocellular carcinoma was positive, while that of hemangioma, metastasis and cholangiocarcinoma was negative. The postcontrast CNR of all tumors except hepatocellular carcinoma increased more than 100%. Qualitative studies showed that tumor conspicuity increased significantly at all sequences except SE, and delineation increased significantly except at SE and postcontrast 2D GRE FS. After Mn-DPDP, GRE more effectively demonstrated tumor conspicuity and image artifact than did SE, and GRE other than 2D FLASH FS was also better than SE for tumor delineation ( $p < 0.05$ ). The sensitivity of all postcontrast images increased and the tumor detection rate at GRE was significantly higher than at SE.

**Conclusion:** Mn-DPDP favorably affects tumor-to-liver contrast, and may be useful in the imaging of focal hepatic tumors, more so with 2D or 3D FLASH pulse sequences than with SE.

**Index words :** Liver, MR

Liver, neoplasms

Magnetic resonance (MR), contrast enhancement

Magnetic resonance (MR), comparative studies

Manganese

Address reprint requests to : Jeong-Min Lee, M.D., Department of Radiology, Chonbuk National University Hospital,  
634-18, Keumam-dong, Chonju-Shi, Chonbuk 561-712, South Korea.  
Tel. 82-63-250-1172 Fax. 82-63-272-0481